Nuclear matter and finite nuclei in an effective chiral model

P. K. Sahu,[1,2,*] K. Tsubakihara,[3] and A. Ohnishi[2]

[1]*Institute of Physics, Sachivalaya Marg, Bhubaneswar 751 005, India*
[2]*Yukawa Institute for Theoretical Physics, Kyoto University, Kyoto 606-8502, Japan*
[3]*Department of Physics, Faculty of Science, Hokkaido University, Sapporo 060-0810, Japan*

We systematically investigate the vacuum stability and nuclear properties in the effective chiral model with higher-order terms in σ. We evaluate the model parameters by considering the saturation properties of nuclear matter as well as the normal vacuum to be globally stable at zero and finite baryon densities. We find parameter sets giving moderate equations of state and apply these models to finite nuclei.

I. INTRODUCTION

Relativistic mean field (RMF) theory is a powerful approach to describing the properties of infinite nuclear matter and finite nuclei simultaneously [1–20]. Although the RMF theory is very successful around the saturation density and in finite nuclei within the range of the model parameters, there are uncertainties regarding the stiffness and the high-density behavior of the equation of state (EOS). Stiffness of EOS can be experimentally probed in heavy-ion collisions [21–25] and giant monopole resonances [26,27] and is crucial in predicting compact astrophysical phenomena. Therefore, it is very important to develop relativistic models with constraints placed on this uncertainty by some symmetries and to investigate bulk properties of nuclear systems. One of the most important symmetries in hadron physics is chiral symmetry. Chiral symmetry is a fundamental symmetry in quantum chromodynamics (QCD) with massless quarks, and its spontaneous breaking generates hadron masses through the chiral condensate $\langle q\bar{q} \rangle$ [28–30], which is considered to be partially restored in dense matter. Thus, theories of quarks and hadrons should respect this essential symmetry in examining dense hadronic matter, and several attempts have been made by including chiral symmetry in relativistic nuclear many-body theories [6–20].

The first RMF model was proposed to deal with the properties of nuclear matter and finite nuclei [1]. In this approach, the meson fields (σ and ω) are treated as the classical limit termed the mean field approximation. The RMF model is extended by introducing the isovector-vector meson ρ and the nonlinear self-coupling terms of mesons to obtain better descriptions of nuclear matter and finite nuclei [2–5]. The significant point of this extension is that its nonlinear terms simulate three-body forces, which is essential to reproduce nuclear matter saturation properties in nonrelativistic calculations. There are several problems with regarding these RMF models as finite-density hadronic field theories. First, these models do not possess chiral symmetry. Although the in-medium nucleon mass is shifted by the σ field and the scalar σ field may be related to the chiral condensate,

the self-energy of σ is not chirally invariant. Second, the vacuum is not stable with respect to the variation of σ in many RMF models. We do not have practical problems in describing nuclear matter and finite nuclei in the mean field treatment where the fluctuation of meson fields is omitted, but the vacuum instability is conceptually problematic.

The effective chiral model is analogous to the RMF model. We start from the ϕ^4 theory, in which spontaneous symmetry breaking is included, and vector mesons are introduced to describe the repulsive potential at high density. When we naïvely introduce the vector meson field into the ϕ^4 theory, however, it is known that the normal vacuum jumps to a chiral restored abnormal vacuum (Lee-Wick vacuum) below the saturation density [6,31]; this problem is referred to as the chiral collapse problem [32]. One of the prescriptions for avoiding this problem is to incorporate a logarithmic term of σ [7–15] in the chiral potential (energy density as a function of σ at zero baryon density). The logarithmic σ potential is first introduced to simulate the scale anomaly in QCD, which is represented by the glueball dilaton field (χ), which couples with the logarithm of σ as $\propto -\chi^4 \log \sigma$ [7–12]. It is also possible to derive it from the strong coupling limit (SCL) of lattice QCD [13–15,33,34]. The logarithmic potential term, $\propto -\log \sigma$, generally prevents the normal vacuum from collapsing and hence it has no instabilities. Also, this model can describe even-even finite nuclei and infinite nuclear matter properties well with inclusion of the vector mesons, their linear couplings to nucleons, and a self-interaction term, $(\omega_\mu \omega^\mu)^2$ [12–15]. In Ref. [12], for example, Schramm applied a chiral SU(3) RMF model with a logarithmic σ potential and the glueball interaction to nuclei over the whole known range assuming axial symmetry, and it was demonstrated that binding energies of spherical and deformed nuclei are well explained, with an accuracy of 0.1%–1%. Although these models have had phenomenological successes and are somewhat based on QCD, one may doubt the validity of the logarithmic potential, as it is divergent when chiral symmetry is restored, $\sigma \to 0$.

Another way to avoid chiral collapse is to introduce a dynamical generation of the isoscalar-vector meson mass through the coupling between scalar and vector mesons [6,16]. Because the vector meson becomes light when chiral symmetry is partially restored, repulsive effects from the vector meson become strong and chiral collapse can be avoided.

_____
*pradip@iopb.res.in

One of the problems with this theoretical treatment is the unrealistically high incompressibility value, $K \gtrsim 700$ MeV. To obtain a moderate value of incompressibility, Sahu *et al.* introduced the higher-order terms of scalar meson, σ^6, and σ^8 [17–19]. In this way, the empirical values of saturation density, binding energy, and incompressibility in symmetric nuclear matter can be reproduced. The advantage of higher-order terms in the chiral potential is that there is freedom to adopt a weaker repulsive vector force in the nuclear interaction, and therefore, there is a choice of desirable incompressibility values. In earlier studies [17–20], the aforementioned model with higher-order terms in scalar-field interactions was used extensively in dense matter as well as hot nuclear matter. In all these works, the vacuum stability at large σ values was not critically examined for all sets of parameters. It has recently been pointed out [13,14] that one of the parameters in a previous study [18] is unstable at large σ. Although several sets of parameters of this model were tabulated, few of them overcome the instability at large σ. Therefore, we are motivated to revisit this model and put stringent constraints on parameters for stability with respect to the σ field.

In this paper, we systematically investigate the vacuum stability and nuclear properties in the effective SU(2) chiral model having higher-order terms in the chiral potential V_σ. The condition of vacuum stability is elucidated in the parameter plane in the model. We calculate the EOS for symmetric nuclear matter with a moderate choice of incompressibility, between 300 and 400 MeV, and effective masses around 0.85 of the nucleon mass, under the constraint of vacuum stability. Parameters are chosen accordingly by constraining these conditions at nuclear saturation points. We also apply our model to finite spherical nuclei and perform a naive dimensional analysis (NDA) to examine the naturalness of the effective Lagrangian.

Throughout the paper, we work in the chiral limit ($m_\pi = 0$) for simplicity. As long as we do not explicitly include π-meson effects in the mean field approximation, the results with finite m_π in nuclear matter and finite nuclei are found to be very similar to those in the chiral limit. We ignore these small differences, as the main aim of this paper is to elucidate the vacuum stability condition in effective chiral models.

The paper is organized as follows: In Sec. II, we present a brief formalism of the effective chiral model. We investigate the properties of nuclear matter and finite nuclei in Sec. III. Basically, we determine the suitable model parameters to explain the saturation properties of nuclear matter as well as the vacuum stability. Then we determine the EOS and the properties of finite nuclei. We also examine the naturalness of the effective Lagrangian using naive dimensional analysis in Sec. III. We summarize our results in Sec. IV.

II. THE FORMALISM OF THE SU(2) EFFECTIVE CHIRAL MODEL

The effective chiral Lagrangian, which includes a dynamically generated mass of the isoscalar-vector field ω_μ that couples to the conserved baryonic current $j_\mu = \bar{\psi}\gamma_\mu\psi$, can

be written as [17,18]

$$\mathcal{L} = \bar{\psi}[i\not{\partial} - g_\sigma(\sigma + i\gamma_5\boldsymbol{\tau}\cdot\boldsymbol{\pi}) - g_\omega\not{\omega} - g_\rho\not{\rho}\cdot\boldsymbol{\tau}]\psi$$
$$+ \tfrac{1}{2}(\partial_\mu\boldsymbol{\pi}\cdot\partial^\mu\boldsymbol{\pi} + \partial_\mu\sigma\,\partial^\mu\sigma) - V_\sigma(\sigma,\boldsymbol{\pi}) - \tfrac{1}{4}F^{\mu\nu}F_{\mu\nu}$$
$$+ \tfrac{1}{2}g_{\sigma\omega}^2 x^2\omega_\mu\omega^\mu - \tfrac{1}{4}\mathbf{G}_{\mu\nu}\cdot\mathbf{G}^{\mu\nu} + \tfrac{1}{2}m_\rho^2\boldsymbol{\rho}_\mu\cdot\boldsymbol{\rho}^\mu. \quad (1)$$

We introduce a chiral-symmetric-type interaction up to eighth order of the meson field, which reads

$$V_\sigma = \frac{C_4 f_\pi^4}{4}\left(\frac{x^2}{f_\pi^2} - 1\right)^2 + \frac{m_\pi^2}{2}x^2 - m_\pi^2 f_\pi\sigma$$
$$+ \frac{C_6 f_\pi^4}{6}\left(\frac{x^2}{f_\pi^2} - 1\right)^3 + \frac{C_8 f_\pi^4}{8}\left(\frac{x^2}{f_\pi^2} - 1\right)^4, \quad (2)$$

where $x^2 = \sigma^2 + \boldsymbol{\pi}^2$; f_π is the pion decay constant; $F_{\mu\nu} \equiv \partial_\mu\omega_\nu - \partial_\nu\omega_\mu$ and $\mathbf{G}_{\mu\nu} \equiv \partial_\mu\boldsymbol{\rho}_\nu - \partial_\nu\boldsymbol{\rho}_\mu + g_{\rho\rho}\boldsymbol{\rho}_\mu \times \boldsymbol{\rho}_\nu$ are the field tensors of isoscalar- and isovector-vector mesons (ω and ρ mesons); and ψ, $\boldsymbol{\pi}$, and σ denote the nucleon isospin doublet, isovector-pseudoscalar pion, and scalar fields, respectively. Coupling constants of the nucleon with the scalar and vector fields are introduced as g_σ, g_ω, and g_ρ, respectively. We work in natural units, where $\hbar = c = k_B = 1$.

The interaction terms of the nucleon and vector meson with the scalar and pseudoscalar mesons generate the masses of the nucleon and vector meson through the spontaneous breaking of chiral symmetry. The masses of the nucleon and vector meson in vacuum are given by

$$M_N = g_\sigma f_\pi, \quad m_\omega = g_{\sigma\omega} f_\pi, \quad (3)$$

where the vacuum expectation value of the σ field is replaced with f_π. The coefficient C_4 is related to the vacuum mass of σ as

$$C_4 = \frac{m_\sigma^2 - m_\pi^2}{2f_\pi^2}. \quad (4)$$

The constant parameters C_6 and C_8 are included in the higher-order self-interaction of the scalar field to describe the desirable values of nuclear matter properties at saturation point. In this work, we consider the chiral limit, where the pion mass m_π is 0. In the mean field treatment we ignore the explicit role of π mesons.

By adopting the mean field approximation, the equations of motion of fields are obtained from the chiral Lagrangian. This approach has been used extensively to evaluate the EOS [21–25] in many of the theoretical models for high-density matter. Using the mean field ansatz in uniform matter, the equations of motion for the vector fields (ω and ρ mesons) are solved as

$$\omega = \frac{g_\omega^2\rho_B^2}{g_{\sigma\omega}^2 x^2} = \frac{g_\omega^2\rho_B^2}{m_\omega^2 Y^2}, \quad R \equiv \rho_0^3 = \frac{g_\rho}{m_\rho^2}(\rho_p - \rho_n), \quad (5)$$

where $Y = \sigma/f_\pi$ is the reduction ratio of the chiral condensate from its vacuum value. Proton and neutron densities (ρ_p and ρ_n) are given as $\rho_\alpha = \gamma[k_F^{(\alpha)}]^3/6\pi^2$, where $k_F^{(\alpha)}$ is the Fermi momentum of the proton ($\alpha = p$) or the neutron ($\alpha = n$), and γ is the spin degeneracy factor, $\gamma = 2$. The baryon density is the sum of the proton and neutron densities, $\rho_B = \rho_p + \rho_n$.

The EOS is calculated from the diagonal components of the conserved total energy-momentum tensor corresponding

to the Lagrangian together with the mean field equation of motion for the fermion field and a mean field approximation for the meson fields. The total energy density (ε) and pressure (P) of the uniform many-nucleon system are given by

$$\varepsilon = \varepsilon_N(M_N^*) + V_\sigma + \frac{g_\omega^2 \rho_B^2}{2m_\omega^2 Y^2} + \frac{1}{2}m_\rho^2 R^2, \tag{6}$$

$$P = P_N(M_N^*) - V_\sigma + \frac{g_\omega^2 \rho_B^2}{2m_\omega^2 Y^2} + \frac{1}{2}m_\rho^2 R^2, \tag{7}$$

$$\varepsilon_N = \sum_{\alpha=p,n} \frac{\gamma}{2\pi^2} \int_0^{k_F^{(\alpha)}} k^2 dk \sqrt{k^2 + M_N^{\star 2}}, \tag{8}$$

$$P_N = \sum_\alpha \frac{\gamma}{6\pi^2} \int_0^{k_F^{(\alpha)}} \frac{k^4 dk}{\sqrt{k^2 + M_N^{\star 2}}}, \tag{9}$$

where $M_N^\star \equiv YM_N = g_\sigma \sigma$ is the effective mass of the nucleon. The free (kinetic) nucleon energy density and pressure, ε_N and P_N, depend on the effective mass M_N^*, as well as on the nuclear density ρ_B.

The equilibrium value of the scalar field (σ) is obtained from the equation of motion, and it is equivalent to the minimum-energy-density condition, $\partial\varepsilon/\partial\sigma = 0$. The equation of motion in terms of Y is given as

$$C_4(1 - Y^2) - C_6(1 - Y^2)^2 + C_8(1 - Y^2)^3$$
$$+ \frac{g_\omega^2 \rho_B^2}{m_\omega^2 f_\pi^4 Y^4} - \frac{g_\sigma \rho_s}{f_\pi^3 Y} = 0, \tag{10}$$

where ρ_s denotes the scalar density, defined as

$$\rho_S = \sum_{\alpha=p,n} \frac{\gamma}{(2\pi)^3} \int_0^{k_F^{(\alpha)}} \frac{M_N^* d^3k}{\sqrt{k^2 + M_N^{*\,2}}}. \tag{11}$$

In previous studies [17–20], the ωN coupling and $\sigma\omega$ coupling were assumed to be the same, $g_\omega = g_{\sigma\omega}$, and the pion decay constant f_π was not introduced explicitly. The energy density is represented by $c_\sigma (= g_\sigma^2/m_\sigma^2)$, $c_\omega = g_\omega^2/m_\omega^2$, and B and C, which are related to the σ^6 and σ^8 coefficients, respectively. In these studies, the implicitly given f_π value is not necessarily the same as the observed one, $f_\pi \simeq 93$ MeV. However, it is possible to map those parameters into the coefficients in the present work by comparing, for example, the energy density, if we do not require the condition $g_\omega = g_{\sigma\omega}$. The relationships of their parameters to the present parameters are given by

$$C_4 = \frac{M_N^2}{2c_\sigma f_\pi^4}, \quad C_6 = \frac{B}{2f_\pi^4 c_\sigma c_\omega}, \quad C_8 = \frac{C}{2f_\pi^4 c_\sigma c_\omega^2 M_N^2}, \tag{12}$$

and $g_\omega = \sqrt{c_\omega}m_\omega$. In the discussion section, we also examine the stability of their Lagrangians.

III. RESULTS AND DISCUSSION

In this section we determine the parameter sets at nuclear matter saturation density. We select the parameters by examining the stability with respect to the σ field. We then use stable parameter sets to find the properties of finite spherical nuclei and examine the naturalness of the effective Lagrangian by performing a naive dimensional analysis. Here we use constants $M_N = 938$ MeV, $f_\pi = 93$ MeV, $m_\omega = 783$ MeV, $m_\rho = 770$ MeV, and $g_\sigma = M_N/f_\pi$.

A. Fixing parameters in symmetric nuclear matter

In the effective chiral model, the chiral symmetry relates the interaction parameters and hadron masses, and reduces the number of parameters, as shown in Eq. (3). In the present treatment, we have five parameters, g_ω, g_ρ, C_4, C_6, and C_8. Here we determine three parameters: the nucleon coupling to the vector field, g_ω, and the coefficients in the scalar potential terms, C_4 and C_6, in symmetric nuclear matter. These parameters are obtained as functions of C_8 and the nucleon effective (Landau) mass $M_N^*(\rho_0)$ by fitting the empirical saturation point (ρ_0, E_0/A), where E_0/A is the binding energy per nucleon at saturation density, $\rho_B = \rho_0$. The saturation point plays a decisive role in finite nuclear binding energies and radii, thus we adjust them to reproduce the finite nuclear property. Moreover, the incompressibility K and the nucleon effective mass $M_N^*(\rho_0)$ are the keys in the EOS around the saturation point, as well as at high densities. The nuclear incompressibility is somewhat uncertain at the saturation point. The desirable values of effective mass and nuclear matter incompressibility are chosen in accordance with recent heavy-ion collision data [21–25]. In our calculation, we have examined several parameter sets corresponding to each incompressibility and effective mass in the ranges 200–400 MeV and (0.8–0.9)M_N [35], respectively, to observe the sensitivity of EOS in the high-density region.

First, we introduce and examine the vacuum stability of the chiral potential as the constraint on the parameters. The vacuum stability condition of the present effective chiral models can be examined as follows. The vacuum energy density is given as V_σ in Eq. (2), which is rewritten as

$$\frac{V_\sigma}{f_\pi^4} = \frac{X^2}{2}f(X), \quad f(X) = \frac{C_8}{4}X^2 + \frac{C_6}{3}X + \frac{C_4}{2}, \tag{13}$$

where $X = (Y^2 - 1)$. In stable cases, V_σ must always be positive in the range $X > -1$ except for the vacuum $X = 0$ (i.e., $\sigma = f_\pi$), at which $V_\sigma = 0$. Provided that $C_8 \geqslant 0$, the stability is ensured when one of the following conditions is satisfied: (1) the discriminant of $f(X)$, $D = (C_6/3)^2 - 4(C_8/4)(C_4/2)$, is negative; (2) the discriminant of $f(X)$ is positive, but the solutions of $f(X) = 0$ are in the range $X \leqslant -1$; or (3) in the case of $C_8 = 0$, $C_6 \geqslant 0$ and $f(-1) > 0$.

By fitting the saturation point, we can fix C_4, C_6, and g_ω as functions of $C_8 \geqslant 0$ and the effective mass at normal density, $Y(\rho_0) = M_N^*/M_N \simeq 0.8$–$0.9$. First, we give $Y(\rho_0)$, then g_ω is uniquely determined. From Eqs. (6) and (7), we find that the enthalpy density is free from V_σ,

$$\varepsilon + P = \frac{g_\omega^2 \rho_B^2}{m_\omega^2 Y^2} + m_\rho^2 R^2 + \varepsilon_N(M_N^*) + P_N(M_N^*) \tag{14}$$

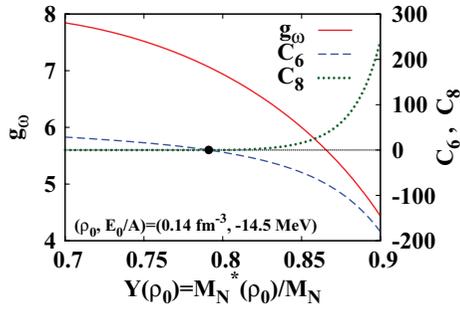$$= \rho_B[M_N - (B/A)] \quad (\rho_B = \rho_0, \rho_p = \rho_n). \tag{15}$$

FIG. 1. (Color online) g_ω as a function of $Y(\rho_0) \equiv M_N^*(\rho_0)/M_N$ (solid line), and C_6 (dashed line) and C_8 (dotted line) values on the vacuum stability boundary.

In Eq. (15), we have used the fact that $P = 0$ at the saturation density. These equations depend on only one parameter, g_ω, and we can fix it from the saturation property. In Fig. 1, we show the g_ω value as a function of $Y(\rho_0) = M_N^*(\rho_0)/M_N$. The energy gain from the σ meson is small for larger values of $Y(\rho_0)$, so the repulsive potential is also chosen to be small to reproduce the binding energy B/A at ρ_0. Thus g_ω is a decreasing function of $Y(\rho_0)$. Next, we give the value of $C_8 \geqslant 0$. For a given set of $[Y(\rho_0), C_8]$, we can solve the condition, $\varepsilon(\rho_0) = \rho_0[M_N - (B/A)]$ and $\partial\varepsilon/\partial\sigma = 0$ at $\rho_B = \rho_0$ [Eq. (10)], with respect to C_4 and C_6.

From these coefficients, we examine the vacuum stability condition. In Fig. 1, we show C_6 and C_8 values on the vacuum stability boundary as a function of $Y(\rho_0)$. These values are equivalent to the minimum C_6 and C_8 values for each $Y(\rho_0)$. At $Y(\rho_0) = 0.781 = Y_{\phi^4}$, ϕ^4 theory is realized, that is, $C_8 = C_6 = 0$. For a larger value of Y at $\rho_B = \rho_0$, repulsion from ω is chosen to be smaller as shown in Fig. 1, and larger repulsion in V_σ is required. This repulsion can be generated by negative C_6 or positive C_8, as $(Y^2 - 1)^3$ and $(Y^2 - 1)^4$ are negative and positive for $Y < 1$, respectively. Thus for small values of C_8, negative C_6 values are required at $Y(\rho_0) > Y_{\phi^4}$, and to maintain the vacuum stability, there exists the minimum value of C_8.

In Fig. 2, we show the vacuum stability region (shaded area) in the $[Y(\rho_0), C_8]$ plane. We have examined the stability of the parameter sets proposed in previous studies [18–20]. We show these parameter sets as open symbols in Fig. 2 and in Table I. Unfortunately, most of the parameter sets that give medium incompressibility (200 MeV < K < 400 MeV) are unstable in vacuum against the variation of σ, denoted "U" in the last column in Table I. Only one parameter set (SJPP-V) fulfills the vacuum stability condition and gives a medium K value.

Parameter sets that we propose and examine in this paper, STO-i ($i = 1, 2, \ldots, 5$), are tabulated in Table I and shown by filled circles in Fig. 2. We have chosen two values of M_N^*/M_N (0.835 and 0.85) and three values of C_8 (20, 40, and 60). The combination $(M_N^*/M_N, C_8) = (0.85, 20)$ is close to the stability boundary, and we do not adopt it. All of these parameters give stable chiral potentials, and the incompressibility values are in the range 200 MeV < $K \lesssim 400$ MeV. We adopt the saturation point $(\rho_0, E_0/A) = [0.14\,\text{fm}^{-3}, -(14.5–14.6)\,\text{MeV}]$, which is found to explain the
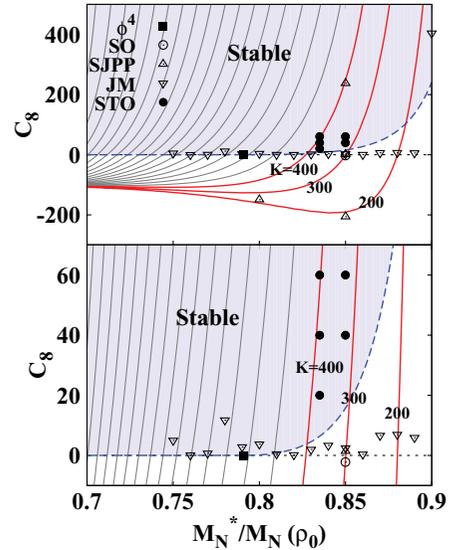

FIG. 2. (Color online) Vacuum stability region (shaded area) and the incompressibility K in the $[Y(\rho_0) = M_N^*(\rho_0)/M_N, C_8]$ plane. Results of several other models [18–20] (open symbols), with ϕ^4 theory (filled square), and with the present model (filled circles).

binding energies of heavy nuclei reasonably well, as discussed in the next subsection.

In Fig. 3, we show the chiral potential V_σ, in STO-5 as an example. We also show the chiral potential in the ϕ^4 theory, TM1 [5], SCL [13,14], and SO [18], for comparison. The chiral potential in STO-5 behaves similarly to that in SO in the region $\sigma < f_\pi$. At larger σ values, unstable parameters give negative chiral potentials in the region $\sigma > f_\pi$, as shown in the SO case. In Fig. 4, we show the EOS in STO-5 in comparison with other EOS. We find that the EOS in STO-5 is reasonably soft, and comparable to those in TM1 and SCL, which explains the bulk properties of finite nuclei.

B. Finite nuclei

In describing finite nuclei, it is numerically preferable to represent the Lagrangian in the shifted field $\varphi \equiv f_\pi - \sigma$ and to separate the σ mass term from the chiral potential V_σ, as the
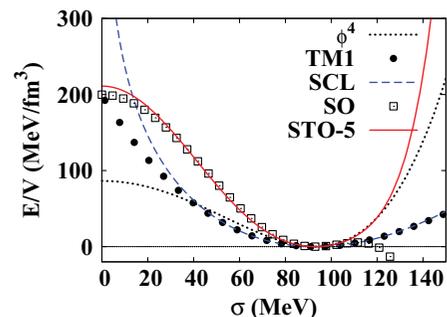

FIG. 3. (Color online) The chiral potential as a function of σ in the ϕ^4 theory (dotted line) and the SCL (dashed line) [13,14], SO (open square) [18], and STO-5 (solid line) models. Results of a nonchiral model, TM1 (filled circles) [5], are also shown for comparison.

TABLE I. Effective chiral model parameter sets. The stability of the model is also reported: S, the vacuum is stable against the variation of σ; U, the vacuum is unstable at large σ.

	M_N^*/M_N	g_ω	C_4	C_6	C_8	K (MeV)	m_σ (MeV)	g_ρ	Stability
ϕ^4	0.781	6.781	37.16	0	0	695.4	801.7	–	S
STO-1	0.850	6.001	35.32	−39.24	40.00	318.5	781.7	3.597	S
STO-2	0.835	6.331	35.37	−25.47	20.00	376.0	782.2	3.467	S
STO-3	0.835	6.328	36.18	−16.77	40.00	389.5	791.1	3.467	S
STO-4	0.835	6.328	37.10	−7.682	60.00	402.3	801.1	3.467	S
STO-5	0.850	6.001	36.09	−30.91	60.00	327.2	790.1	3.467	S
SO	0.85	5.610	33.60	−74.380	−2.200	335.300	762.3		U
SJPP2003-I	0.85	5.598	25.84	−159.000	−206.200	210.000	668.6		U
SJPP2003-II	0.85	5.598	33.73	−73.210	1.405	300.000	763.8		U
SJPP2003-III	0.85	5.598	42.72	24.260	237.400	380.000	859.7		S
SJPP2003-IV	0.80	6.532	26.94	−92.050	−149.400	300.000	682.6		U
SJPP2003-V	0.90	4.047	98.28	906.200	4270.000	300.000	1304.0		S
JM2009-1	0.75	7.106	38.71	17.030	4.998	1142.000	818.3	4.39	S
JM2009-2	0.76	7.016	37.87	9.958	0.085	1010.000	809.3	4.40	S
JM2009-3	0.77	6.908	37.63	6.021	0.713	897.200	806.8	4.41	S
JM2009-4	0.78	6.796	38.13	7.567	11.750	815.000	812.2	4.42	S
JM2009-5	0.79	6.669	37.10	−3.428	2.817	710.400	801.1	4.43	S
JM2009-6	0.80	6.531	36.80	−9.658	3.751	630.700	797.8	4.44	S
JM2009-7	0.81	6.380	36.20	−19.340	0.482	555.500	791.4	4.45	U
JM2009-8	0.82	6.212	35.75	−29.030	0.179	490.800	786.4	4.46	U
JM2009-9	0.83	6.048	35.37	−38.570	1.966	439.300	782.2	4.47	U
JM2009-10	0.84	5.830	34.71	−53.690	3.313	383.800	774.8	4.48	U
JM2009-11	0.85	5.605	33.81	−72.440	2.481	335.800	764.8	4.49	U
JM2009-12	0.86	5.358	32.61	−96.850	0.383	292.200	751.1	4.49	U
JM2009-13	0.87	5.09	31.26	−125.400	6.621	254.400	735.4	4.50	U
JM2009-14	0.88	4.780	29.11	−166.800	6.942	217.900	709.7	4.51	U
JM2009-15	0.89	4.435	26.05	−224.50	5.910	183.500	671.2	4.52	U
JM2009-16	0.90	4.049	28.83	−191.300	404.300	173.400	706.2	4.53	S

boundary condition is given as $\varphi \to 0$ at $r \to \infty$. In addition, it is necessary to include the photon field, which represents the Coulomb potential. Here we take the static and mean field approximation for boson fields, then the RMF Lagrangian can be written as follows:

$$\mathcal{L}_\chi^{\text{RMF}} = \overline{\psi}[i\partial\!\!\!/ - M_N^*(\varphi) - \gamma^0 U_v(\omega, R, A)]\psi - \tfrac{1}{2}(\nabla\varphi)^2$$
$$- \tfrac{1}{2}m_\sigma^2\varphi^2 - V_\varphi(\varphi) + \tfrac{1}{2}(\nabla\omega)^2 + \tfrac{1}{2}M_\omega^2(\varphi)\omega^2$$
$$+ \tfrac{1}{2}(\nabla R)^2 + \tfrac{1}{2}m_\rho^2 R^2 + \tfrac{1}{2}(\nabla A)^2, \quad (16)$$
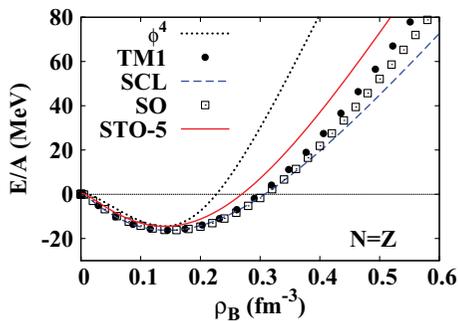

FIG. 4. (Color online) Energy per nucleon as a function of baryon density. For definition of lines and symbols, see the caption to Fig. 3.

where

$$M_N^*(\varphi) = M_N - g_\sigma\varphi, \quad M_\omega^2(\varphi) = g_{\sigma\omega}^2(f_\pi - \varphi)^2, \quad (17)$$

$$U_v(\omega, R, A) = g_\omega\omega + g_\rho\tau_3 R + e\frac{1 + \tau_3}{2}A, \quad (18)$$

$$V_\varphi \equiv V_\sigma - \frac{1}{2}m_\sigma^2\varphi^2. \quad (19)$$

The field equations of motion derived from this Lagrangian read

$$[-i\alpha \cdot \nabla + \beta M^* + U_v]\psi = \varepsilon_i\psi, \quad (20)$$

$$(-\triangle + m_\sigma^2)\varphi = g_\sigma\rho_S - \frac{dV_\varphi}{d\varphi} - g_{\sigma\omega}^2(f_\pi - \varphi)\omega^2, \quad (21)$$

$$(-\triangle + m_\omega^2)\omega = g_\omega\rho_B + g_{\sigma\omega}^2\varphi(2f_\pi - \varphi)\omega, \quad (22)$$

$$(-\triangle + m_\rho^2)R = g_\rho\rho_\tau, \quad (23)$$

$$-\triangle A = e\rho_B^p, \quad (24)$$

where $\rho_S = \rho_S^p + \rho_S^n$, $\rho_B = \rho_B^p + \rho_B^n$, and $\rho_\tau = \rho_B^p - \rho_B^n$ denote the scalar, baryon, and isospin densities of nucleons, respectively. The total energy is given by the integral of the

energy density, given as

$$
\begin{aligned}
E = {} & \sum_{i\kappa\alpha} n_{i\kappa\alpha}^{\mathrm{occ}} \varepsilon_{i\kappa\alpha} \\
& - \frac{1}{2} \int \left\{ -g_\sigma \varphi \rho_S + g_\omega \omega \rho_B + g_\rho R \rho_\tau + e^2 A \rho_B^p \right\} d\mathbf{r} \\
& + \int \left\{ V_\varphi - \frac{1}{2} \varphi \frac{dV_\varphi}{d\varphi} - \frac{g_{\sigma\omega}^2}{2} \varphi \left(f_\pi - \varphi \right) \omega^2 \right\} d\mathbf{r}, \quad (25)
\end{aligned}
$$

where we use Eqs. (20)–(24) to calculate second-order derivatives of meson fields. Nucleon single-particle states are specified by the radial quantum number i, isospin $\alpha(=p, n)$, and angular momentum quantum number, $\kappa = l$ [$\kappa = -(l+1)$], for $j = l - \frac{1}{2}$ ($j = l + \frac{1}{2}$). The number of occupied nucleons is represented by $n_{i\kappa\alpha}^{\mathrm{occ}}$, which is equal to $2|\kappa| = 2j + 1$ for filled single-particle states. We solve the self-consistent coupled equations (20)–(24) by iteration until the convergence of total energy is achieved. In this work, we assume that the nuclei under consideration are spherical, then the nucleon wave functions are expanded in spherical harmonic basis as follows:

$$
\psi_{\alpha i\kappa m} = \begin{pmatrix} i \left[G_{i\kappa}^\alpha / r \right] \Phi_{\kappa m} \\ - \left[F_{i\kappa}^\alpha / r \right] \Phi_{-\kappa m} \end{pmatrix} \zeta_\alpha, \quad (26)
$$

$$
\rho_B^\alpha = \sum_{i\kappa} \left(\frac{n_{i\kappa\alpha}^{\mathrm{occ}}}{4\pi r^2} \right) \left[\left| G_{i\kappa}^\alpha(r) \right|^2 + \left| F_{i\kappa}^\alpha(r) \right|^2 \right], \quad (27)
$$

$$
\rho_S^\alpha = \sum_{i\kappa} \left(\frac{n_{i\kappa\alpha}^{\mathrm{occ}}}{4\pi r^2} \right) \left[\left| G_{i\kappa}^\alpha(r) \right|^2 - \left| F_{i\kappa}^\alpha(r) \right|^2 \right], \quad (28)
$$

where ζ_α represents the isospin wave function, $\alpha = p, n$.

In comparing the calculated results in mean field models with the experimental binding energies and charge radii, we have to take account of several corrections. In this work, we consider the center-of-mass (CM) kinetic energy correction on the total energy, and the CM and nucleon size correction on the nuclear charge root-mean-square (rms) radius, in the same way as adopted in Ref. [5]. The CM kinetic energy is assumed to be

$$
E_{\mathrm{ZPE}} = \frac{\langle \mathbf{P}_{\mathrm{CM}}^2 \rangle}{2AM_N} \simeq \frac{3}{4}\hbar\omega = \frac{3}{4} 41 A^{-1/3}, \quad (29)
$$

where $\mathbf{P}_{\mathrm{CM}} = \sum_i \mathbf{p}_i$ is the CM momentum. This correction gives an exact result when the state is represented by a harmonic-oscillator wave function, and we assume that it also applies to RMF wave functions. The CM correction on the proton rms radius is written as

$$
\delta\langle r_p^2 \rangle = -2\langle \mathbf{R}_{\mathrm{CM}} \cdot \mathbf{R}_p \rangle + \langle \mathbf{R}_{\mathrm{CM}}^2 \rangle
$$

$$
\simeq \begin{cases} -\dfrac{3\hbar}{2AM_N\omega} & \text{(for heavy nuclei),} \\[2ex] -\dfrac{2\langle r_p^2 \rangle}{A} + \dfrac{\langle r_m^2 \rangle}{A} & \text{(for light nuclei),} \end{cases} \quad (30)
$$

where $\mathbf{R}_p = \sum_{i \in p} \mathbf{r}_i / Z$ is the proton CM position, and $\langle r_p^2 \rangle$ and $\langle r_m^2 \rangle$ represent the proton and matter mean square radii, respectively. We assume again that harmonic-oscillator results apply to heavy nuclei. For light nuclei, we evaluate the correction in RMF wave functions, and we consider only the

direct-term contributions. The charge rms radius is obtained by including the finite-size effects of protons and neutrons,

$$
\langle r_{\mathrm{ch}}^2 \rangle = \langle r_p^2 \rangle + \langle r_{\mathrm{size}}^2 \rangle_p - \frac{N}{Z}\langle r_{\mathrm{size}}^2 \rangle_n, \quad (31)
$$

where $\langle r_{\mathrm{size}}^2 \rangle_\alpha$ denotes the size of the proton or neutron and is equal to $(0.862 \text{ fm})^2$ or $(0.336 \text{ fm})^2$, respectively. We evaluate the binding energies and charge rms radii with these corrections, and the pairing energies for open-shell nuclei are neglected.

In describing finite nuclei, the isospin-dependent interaction is an important ingredient. In uniform nuclear matter, we can obtain the symmetric energy coefficient a_{sym} by expanding the energy density around the symmetric nuclear matter,

$$
a_{\mathrm{sym}} = \frac{g_\rho^2 k_F^3}{3\pi^2 m_\rho^2} + \frac{k_F^2}{6\sqrt{k_F^2 + M_N^{\star 2}}}, \quad (32)
$$

where $k_F = (6\pi^2 \rho_B / \gamma)^{1/3} (\rho_B = \rho_p + \rho_n, \gamma = 4)$ is the Fermi momentum in symmetric nuclear matter. To reproduce the empirical value of the symmetry energy coefficient, $a_{\mathrm{sym}} = 32 \pm 6$ MeV [35], Eq. (32) gives $g_\rho = 4.625$ and $M^* = 0.85M$. In the present work, we have fixed g_ρ by fitting the binding energies of heavy nuclei. We find that $g_\rho \simeq 3.5$ is appropriate.

We have tuned the model parameters so as to explain the binding energies of heavy nuclei. In Table II, we tabulate finite nuclei results. We also summarize the STO parameter sets and the resulting incompressibility in Table I. The binding

TABLE II. Calculated results for the saturation property of symmetric nuclear matter, B/A, and charge rms radii of stable nuclei.

|	STO-1	STO-2	STO-3	STO-4	STO-5	Exp.
Saturation property						
ρ_0	0.14	0.14	0.14	0.14	0.14	
E_0	-14.6	-14.5	-14.6	-14.6	-14.5	
K	318.5	376.0	389.5	402.3	327.2	
B/A						
^{12}C	9.38	9.40	9.37	9.26	9.30	7.68
^{16}O	10.9	10.9	10.9	10.7	10.8	7.98
^{28}Si	9.53	9.57	9.87	9.47	9.47	8.45
^{40}Ca	9.91	9.85	9.56	9.80	9.86	8.55
^{48}Ca	9.73	9.74	9.74	9.68	9.70	8.67
^{90}Zr	9.13	9.11	9.15	9.09	9.11	8.71
^{116}Sn	8.83	8.81	8.85	8.80	8.81	8.52
^{196}Pb	7.87	7.85	7.91	7.86	7.86	7.87
^{208}Pb	7.87	7.85	7.91	7.86	7.87	7.87
Charge rms radii						
^{12}C	2.27	2.27	2.27	2.27	2.28	2.46
^{16}O	2.44	2.44	2.44	2.44	2.44	2.74
^{28}Si	2.95	2.94	2.95	2.95	2.95	3.09
^{40}Ca	3.30	3.30	3.30	3.30	3.30	3.45
^{48}Ca	3.39	3.39	3.39	3.39	3.39	3.45
^{90}Zr	4.21	4.20	4.20	4.20	4.21	4.26
^{116}Sn	4.59	4.59	4.59	4.59	4.60	4.63
^{196}Pb	5.48	5.47	5.47	5.47	5.48	–
^{208}Pb	5.56	5.55	5.54	5.54	5.56	5.50
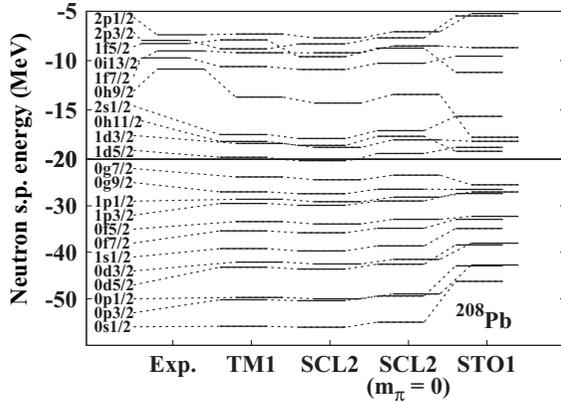
FIG. 5. Neutron single-particle levels of ^{208}Pb in the models TM1, SCL2, SCL2 in the chiral limit, and STO.

energy per nucleon in heavy nuclei and the incompressibility parameters are in the acceptable range. On the contrary, we cannot reproduce the binding energies of light nuclei simultaneously with those of heavy nuclei. Calculated values of charge rms radii underestimate the data as long as we vary the ρ_0 value in the acceptable range, $\rho_0 = 0.14$–0.16 fm^{-3}.

We show the results obtained in the chiral limit ($m_\pi = 0$), but the results are not modified much with a finite pion mass in the mean field approximation. This is examined in an RMF model with the chiral SU(2) logarithmic potential (SCL2) with finite m_π [13]. In Fig. 5, we present the calculated neutron single-particle levels of ^{208}Pb in the chiral limit. Not only in the level structure but also in their energies, there is little difference between the SCL2 results with finite and those with zero pion masses. Therefore in the mean field approximation, we can safely discuss the properties of the RMF Lagrangian in the chiral limit.

We also show in Fig. 5 that the present model (STO-1) shows smaller ls splitting compared with other RMF models, owing to the large effective nucleon masses. One of the original motivations for using RMF models for nuclei was the large ls splitting naturally generated from the large scalar and vector potentials additively. In the recently developed chiral RMF models [12,13], ls splittings are evaluated to be smaller than the empirical values. This may suggest the need to include explicit pion effects. There is some discussion regarding the contribution to ls splitting [36] where one-pion-exchange tensor force and two-pion exchange with the excitation of virtual $\Delta(1\,232)$ isobars are taken into account to explain the ls splitting property of the nucleon and the hyperon simultaneously. The ls-like roles of the tensor force or pions in light nuclei are also discussed [37]. We have not taken account of these pion effects in our present calculations, thus π treatment may be required to resolve the ls splitting problem in chiral RMF models and effective chiral models.

C. Naive dimensional analysis

The present STO model is a kind of effective field theory, contains higher-order terms, and is nonrenormalizable. Thus it would be valuable to examine the naturalness in a naive dimensional analysis [38–42]. It is found that the loop

contributions with the momentum cutoff $\Lambda \sim 1$ GeV generate the following terms with dimensionless coefficients C_{lmnp} of order unity [38–40,42]:

$$\mathcal{L}_{\text{int}} \sim \sum_{l,m,n,p} \frac{C_{lmnp}}{m!\,n!\,p!} \left(\frac{\bar{\psi}\,\Gamma\,\psi}{f_\pi^2 \Lambda} \right)^l$$
$$\times \left(\frac{\varphi}{f_\pi} \right)^m \left(\frac{\omega}{f_\pi} \right)^n \left(\frac{\rho}{f_\pi} \right)^p (f_\pi \Lambda)^2, \qquad (33)$$

where Γ denotes the γ and $\tau/2$ when necessary.

An effective theory having terms in Eq. (33) is considered to hold naturalness when all the dimensionless coefficients C_{lmnp} are of order unity. In the present effective Lagrangian, we obtain the following dimensionless coefficients:

$$C_{1100} = \frac{f_\pi g_\sigma}{\Lambda} = \frac{M_N}{\Lambda} \sim 0.94,$$

$$C_{1010} = \frac{f_\pi g_\omega}{\Lambda} \sim 0.56,$$

$$C_{1001} = \frac{2 f_\pi g_\rho}{\Lambda} \sim 0.64,$$

$$C_{0120} = -\frac{2 g_{\sigma\omega}^2 f_\pi^2}{\Lambda^2} = -\frac{2 m_\omega^2}{\Lambda^2} \sim 1.2,$$

$$C_{0220} = \frac{2 g_{\sigma\omega}^2 f_\pi^2}{\Lambda^2} = \frac{2 m_\omega^2}{\Lambda^2} \sim 1.2,$$

$$C_{0300} = \frac{f_\pi^2}{\Lambda^2}\, 3! \left(\frac{4}{3} C_6 - C_4 \right) \sim -4, \qquad (34)$$

$$C_{0400} = \frac{f_\pi^2}{\Lambda^2}\, 4! \left(2C_8 - 2C_6 + \frac{1}{4} C_4 \right) \sim 40,$$

$$C_{0500} = \frac{f_\pi^2}{\Lambda^2}\, 5!\, (-4C_8 + C_6) \sim -280,$$

$$C_{0600} = \frac{f_\pi^2}{\Lambda^2}\, 6! \left(3C_8 - \frac{1}{6} C_6 \right) \sim 1200,$$

$$C_{0700} = -\frac{f_\pi^2}{\Lambda^2}\, 7! C_8 \sim -2600,$$

$$C_{0800} = \frac{f_\pi^2}{\Lambda^2}\, \frac{8!}{8} C_8 \sim 2600.$$

We show the results in STO-5 and adopt $\Lambda = 1$ GeV. We find that the meson-nucleon and $\sigma\omega$ couplings are natural, but the self-interaction coefficients in σ are not natural.

IV. SUMMARY AND CONCLUSIONS

In this paper, we have investigated the properties of nuclear matter and finite nuclei in the effective chiral model with σ^6 and σ^8 terms. The nucleon-vector meson coupling is found to be uniquely determined as a function of the effective mass at normal nuclear matter density, $Y(\rho_0) \equiv M_N^*(\rho_0)/M_N$, and we have specified the region of stability in the $[Y(\rho_0), C_8]$ plane, where C_8 is the coefficient of the σ^8 term. We can find the parameter sets that satisfy the vacuum stability condition and result in moderate incompressibility, $K = (200 - 400)$ MeV. The incompressibility is found to be dominated by the nucleon

effective mass, and $M_N^*(\rho_0)/M_N \gtrsim 0.83$ is necessary to obtain a moderate K, as far as vacuum stability is required.

The obtained effective chiral model with higher-order terms in σ is applied to finite nuclei for the first time. It can explain the binding energies of heavy nuclei (Sn and Pb) reasonably well, whereas it overestimates the binding energies of light nuclei. This may be because the nucleon-vector meson coupling is small, $g_{\omega N} \sim 6$, compared with other RMF models that explain nuclear binding energies over a wide mass range, such as NL1 ($g_{\omega N} = 13.285$) [2,3], NL3 ($g_{\omega N} = 12.868$) [4], TM1 ($g_{\omega N} = 12.6139$) [5], and SCL ($g_{\omega N} = 13.02$) [33,34]. The smaller $g_{\omega N}$ value is compensated at higher densities where chiral symmetry is partially restored and the ω mass decreases, but light nuclei are more sensitive to the EOS at lower densities.

We have also performed a naïve dimensional analysis [38–42] of the present model. A moderate K value, around 300 MeV, requires the σ^8 coefficient $C_8 \gtrsim 20$ as shown in Fig. 2. This value corresponds to $C_{0800} \gtrsim 870$, and the

model cannot hold naturalness. To construct effective chiral models having moderate incompressibility, vacuum stability, and naturalness simultaneously, it would be necessary to introduce types of interaction terms other than polynomial forms of σ. Work in this direction would be valuable for our understanding of the chiral properties of the QCD vacuum.

[1] B. D. Serot and J. D. Walecka, Adv. Nucl. Phys. **16**, 1 (1986).

[2] P.-G. Reinhard, M. Rufa, J. Maruhn, W. Greiner, and J. Friedrich, Z. Phys. A **323**, 13 (1986).

[3] S.-J. Lee, J. Fink, A. B. Balantekin, M. R. Strayer, A. S. Umar, P. G. Reinhard, J. A. Maruhn, and W. Greiner, Phys. Rev. Lett. **57**, 2916 (1986).

[4] G. A. Lalazissis, J. König, and P. Ring, Phys. Rev. C **55**, 540 (1997).

[5] Y. Sugahara and H. Toki, Nucl. Phys. **A579**, 557 (1994).

[6] J. Boguta, Phys. Lett. **B120**, 34 (1983).

[7] R. J. Furnstahl and B. D. Serot, Phys. Lett. **B316**, 12 (1993).

[8] E. K. Heide, S. Rudaz, and P. J. Ellis, Nucl. Phys. **A571**, 713 (1994).

[9] I. Mishustin, J. Bondorf, and M. Rho, Nucl. Phys. **A555**, 215 (1993).

[10] P. Papazoglou, J. Schaffner, S. Schramm, D. Zschiesche, H. Stöcker, and W. Greiner, Phys. Rev. C **55**, 1499 (1997).

[11] P. Papazoglou, S. Schramm, J. Schaffner-Bielich, H. Stöcker, and W. Greiner, Phys. Rev. C **57**, 2576 (1998).

[12] S. Schramm, Phys. Rev. C **66**, 064310 (2002).

[13] K. Tsubakihara and A. Ohnishi, Prog. Theor. Phys. **117**, 903 (2007).

[14] K. Tsubakihara, H. Maekawa, and A. Ohnishi, Eur. Phys. J. A **33**, 295 (2007).

[15] K. Tsubakihara, H. Maekawa, H. Matsumiya, and A. Ohnishi, arXiv:0909.5058 [nucl-th].

[16] P. K. Sahu, R. Basu, and B. Datta, Astrophys. J. **416**, 267 (1993).

[17] P. K. Sahu, Phys. Rev. C **62**, 045801 (2000).

[18] P. K. Sahu and A. Ohnishi, Prog. Theor. Phys. **104**, 1163 (2000).

[19] P. K. Sahu, T. K. Jha, K. C. Panda, and S. K. Patra, Nucl. Phys. **A733**, 169 (2004).

[20] T. K. Jha and H. Mishra, Phys. Rev. C **78**, 065802 (2008).

[21] P. Danielewicz, R. Lacey, and W. G. Lynch, Science **298**, 1592 (2002).

[22] P. K. Sahu and W. Cassing, Nucl. Phys. **A712**, 357 (2002).

[23] P. K. Sahu, W. Cassing, U. Mosel, and A. Ohnishi, Nucl. Phys. **A672**, 376 (2000).

[24] P. K. Sahu, A. Hombach, W. Cassing, M. Effenberger, and U. Mosel, Nucl. Phys. **A640**, 493 (1998).

[25] M. Isse, A. Ohnishi, N. Otuka, P. K. Sahu, and Y. Nara, Phys. Rev. C **72**, 064908 (2005).

[26] J. P. Blaizot, Phys. Rep. **64**, 171 (1980).

[27] D. H. Youngblood, H. L. Clark, and Y. W. Lui, Phys. Rev. Lett. **82**, 691 (1999).

[28] Y. Nambu and G. Jona-Lasino, Phys. Rev. **122**, 345 (1961).

[29] Y. Nambu and G. Jona-Lasino, Phys. Rev. **124**, 246 (1961).

[30] T. Hatsuda and T. Kunihiro, Phys. Rep. **247**, 221 (1994).

[31] T. D. Lee and G. C. Wick, Phys. Rev. D **9**, 2291 (1974).

[32] A. W. Thomas, P. A. M. Guichon, D. B. Leinweber, and R. D. Young, Prog. Theor. Phys. Suppl. **156**, 124 (2004).

[33] N. Kawamoto and J. Smit, Nucl. Phys. **B192**, 100 (1981).

[34] N. Kawamoto, K. Miura, A. Ohnishi, and T. Ohnuma, Phys. Rev. D **75**, 014502 (2007).

[35] P. Moller, W. D. Myers, W. J. Swiatecki, and J. Treiner, At. Data Nucl. Data Tables **39**, 225 (1988).

[36] N. Kaiser and W. Weise, Nucl. Phys. **A804**, 60 (2008).

[37] T. Myo, K. Kato, and K. Ikeda, Prog. Theor. Phys. **113**, 763 (2005); A. Isshiki, K. Naito, and A. Ohnishi, *ibid.* **114**, 573 (2005).

[38] A. Manohar and H. Georgi, Nucl. Phys. **B234**, 189 (1984).

[39] H. Georgi and L. Randall, Nucl. Phys. **B276**, 241 (1986).

[40] H. Georgi, Phys. Lett. **B298**, 187 (1993).

[41] K. Saito, K. Tsushima, and A. W. Thomas, Phys. Lett. **B406**, 287 (1997).

[42] R. J. Furnstahl, B. D. Serot, and H. B. Tang, Nucl. Phys. **A615**, 441 (1997); [Erratum-*ibid.* **A640**, 505 (1998)].